Available online at www.sciencedirect.com
ScienceDirect
Journal of Structural Biology 159 (2007) 523–528
Journal of Structural Biology
www.elsevier.com/locate/yjsbi

Crystallization Notes

Crystal structure of SAM-dependent *O*-methyltransferase from pathogenic bacterium *Leptospira interrogans*

Xiaowei Hou [a,b], Yanli Wang [a], Zhongwei Zhou [c], Shilai Bao [c], Yajing Lin [a], Weimin Gong [a,b,*]

[a] *National Laboratory of Biomacromolecules, Institute of Biophysics, Chinese Academy of Sciences, Beijing 100101, PR China*
[b] *School of Life Sciences, University of Science and Technology of China, Hefei, Anhui 230026, PR China*
[c] *Key Laboratory of Molecular and Developmental Biology, Institute of Genetics and Developmental Biology, Chinese Academy of Sciences, Beijing 100101, PR China*

Received 11 November 2006; received in revised form 17 April 2007; accepted 19 April 2007
Available online 30 April 2007

Abstract

The *S*-adenosylmethionine (SAM)-dependent *O*-methyltransferase from *Leptospira interrogans* (*Li*OMT) expressed by gene *LA0415* belongs to the Methyltransf_3 family (Pfam PF01596). In this family all of the five bacterial homologues with known function are reported as SAM-dependent *O*-methylstransferases involved in antibiotic production. The crystal structure of *Li*OMT in complex with *S*-adenosylhomocysteine reported here is the first bacterial protein structure in this family. The *Li*OMT structure shows a conserved SAM-binding region and a probable metal-dependent catalytic site. The molecules of *Li*OMT generate homodimers by N-terminal swapping, which assists the pre-organization of the substrate-binding site. Based on the sequence and structural analysis, it is implied by the catalytic and substrate-binding site that the substrate of *Li*OMT is a phenolic derivative, which probably has a large ring-shaped moiety.

Keywords: Methyltransferase; SAM-dependent; Crystal; Structure; *Leptospira interrogans*

1. Introduction

Methylation is an important and ubiquitous biological process for all organisms. Most of methyltransferases that catalyze the methylation process utilize *S*-adenosylmethionine (SAM) as a methyl donor, yielding the product *S*-adenosylhomocysteine (SAH) (Fontecave et al., 2004). Substrates of SAM-dependent methyltransferases (MTs) include DNA, RNA, protein, lipid, and small molecules as methyl acceptors. When the atom targeted for methylation is oxygen, the SAM-dependent *O*-methyltransferases are termed OMTs.

Leptospira interrogans is a widespread pathogenic bacterium specific to mammals. Infection can cause kidney damage, meningitis, liver failure, and respiratory distress in severe cases. After whole-genome sequencing of *L. interrogans* (Ren et al., 2003), the product of gene *LA0415* was annotated as a SAM-dependent *O*-methyltransferase (for simplicity the protein will be referred as *Li*OMT) and assigned to the Methyltransf_3 family (Pfam PF01596) without substrate information. This family includes caffeoyl-CoA *O*-methyltransferase (CCoAOMT) that is involved in plant defense (Zhong et al., 1998), catechol *O*-methyltransferase (COMT) that plays an import role in the central nervous system in the mammalian organism (Vidgren et al., 1994), and a family of bacterial OMTs that may be involved in antibiotic production (Hara and Hutchinson, 1992; Pospiech et al., 1996; Wu et al., 2000; Haydock et al., 2005; Li et al., 2006). In this family, five bacterial homologues are known to function in the production of

* Corresponding author. Address: National Laboratory of Biomacromolecules, Institute of Biophysics, Chinese Academy of Sciences, Beijing 100101, PR China. Fax: +86 10 6488 8513.
E-mail address: wgong@ibp.ac.cn (W. Gong).

1047-8477/$ - see front matter © 2007 Elsevier Inc. All rights reserved.
doi:10.1016/j.jsb.2007.04.007

antibiotics. The closest of the five homologues, SafC from *Myxococcus xanthus*, is essential for the biosynthesis of the polypeptide saframycin Mx1, which can work as DNA-binding antibiotic and antitumor agent (Pospiech et al., 1996). Cross-feeding experiment indicated that SafC provides methylated tyrosine derivatives before they become the substrates for the peptide synthetase (Pospiech et al., 1996). The other four homologues are proposed to be responsible for methylating the hydroxyl oxygen atom on the α-carbon of marcolides (Hara and Hutchinson, 1992; Wu et al., 2000; Haydock et al., 2005; Li et al., 2006).

Here, we report the crystal structure of *Li*OMT complexed with the copurified SAH, which is the first bacterial OMT structure in the Pfam family PF01596. The structure of *Li*OMT presents good structural similarity with CCoAOMT from alfalfa and COMT from rat. *Li*OMT resembles these two structures in SAM-binding region, which is structurally conserved throughout most of MTs. Specifically *Li*OMT shows conservation with CCoAOMT and COMT in the catalytic site which is reported to require a divalent metal ion to assist the binding of the hydroxyl bearing substrate. (Schubert et al., 2003). The *Li*OMT structure possesses unique features of the substrate-binding region and the swapped N-terminal dimerization interface. The substrate-binding site shows higher sequence similarity within the bacterial homologues rather than with CCoAOMT and COMT. The three-dimensional structure combined with the primary sequence analysis suggests that the substrate of *Li*OMT is a phenolic derivative that probably has a large ring-shaped moiety as the tail. The structure of *Li*OMT also provides insight into the structures of bacterial OMTs related to the antibiotic production in this specific protein family.

2. Materials and methods

2.1. Protein expression and purification

The gene *LA0415* was cloned into the NdeI and XhoI sites of a pET22b (+) vector (Novagen), and it was expressed in *Escherichia coli* strain BL21 (DE3). Cells were grown at 37 °C in 2L LB medium containing 50 μg/ml ampicillin until $OD_{600} = 0.8$, then added isopropyl-β-D-thiogalactoside (IPTG) to final concentration of 0.5 mM and induced at 20 °C for overnight. Cells were harvested by centrifugation, washed by PBS, and stored at −20 °C. Cell pellets were thawed on ice and lysed by sonication in NaCl-free lysis buffer (20 mM Tris–HCl, pH 8.5, 10 mM imidazole, and 1 mM PMSF) because expressed *Li*OMT precipitated in the presence of NaCl. After centrifugation, the supernatant was loaded onto a Ni^{2+}-affinity column equilibrated with binding buffer (20 mM Tris–HCl, pH 8.5, 10 mM imidazole), washed with 10-column volume of binding buffer, 10-column volume of wash buffer (20 mM Tris–HCl, pH 8.5, 25 mM imidazole), then the protein was eluted with elution buffer (20 mM Tris–HCl, pH 8.5, 300 mM imidazole). The purified protein was concentrated to approximately 20 mg ml^{-1} in buffer (20 mM Tris–HCl pH 8.5) to be used for crystallization.

2.2. Crystallization and data collection

Crystallization was carried out at 277 K using the hanging-drop vapor diffusion method. Each hanging drop is a mixture of 1 μl of protein and an equal volume reservoir solution. Initial crystals were obtained using screen kits from Hampton Research (crystal screen I and II) with the condition 0.5 M lithium sulfate monohydrate, 15% w/v polyethylene glycol 8000. The best diffracting crystals were obtained in a condition with 0.05–0.4 M lithium sulfate monohydrate, 8–10% w/v polyethylene glycol 8000, 0.1 M MES pH 6.5. X-ray diffraction data were collected on a Rigaku R-AXIS IV++ imaging-plate system with a Rigaku FRE Cu rotating-anode generator in Institute of Biophysics, Chinese Academy of Sciences. During the data collection, the crystal was maintained at 100 K using nitrogen gas with cryoprotection (0.4 M lithium sulfate monohydrate, 8–10% w/v polyethylene glycol 8000, 0.1 M MES pH 6.5 and 15% polyethylene glycol 400). The crystal belongs to the space group $P222_1$. The diffraction data were processed and scaled with the HKL2000 suite of program (Otwinowski and Minor, 1997). Data processing statistics are given in Table 1.

2.3. Structure determination

The structure was solved by molecular replacement with the PHASER (Storoni et al., 2004) program, using the CCoAOMT monomer (PDB ID: 1SUI) as the search model. The solution suggested three molecules in the asymmetric unit. Model refinement involved manual adjusting in Coot (Emsley and Cowtan, 2004), rigid and restrained refinement in Refmac5 (Murshudov et al., 1997). NCS restraints among three molecules of an asymmetric unit were applied during the refinement. Water molecules, polyethylene glycol and four sulfate ions were included near the end of refinement, followed by manual modification in the graphics program Coot. The final R_{cryst} and R_{free} factors are 0.213 and 0.243, respectively. The stereochemical quality of the final model was checked by procheck (Laskowski et al., 1993). Refinement statistics and geometry are presented in Table 1.

3. Results and discussion

3.1. Overall structure of LiOMT

There are three *Li*OMT molecules in the asymmetric unit, named molecule A, B, and C, respectively. The final model consists of the full-length of *Li*OMT followed by a few residues in the His-Tag. Met1, Arg2 and Ala38-Ala40 in molecule A, Met1 and Ala40 in molecule B as well as Met1 and Arg2 in molecule C are not built due to the weak electron density. The refinement statistics of the final

Table 1
Data collection and structure refinement statistics

Data collection	
Space group	$P222_1$
Unit cell dimensions (Å) and angles (°)	$a, b, c = 157.81, 60.33, 138.23$ $\alpha = \beta = \gamma = 90$
Molecules per asymmetric unit	3
Resolution range (Å)	50–2.3 (2.38–2.30)
No. of total reflections	108684
No. of unique reflections	59487
Completeness (%)	96.1 (97.6)
I/σ	11.00
R_{merge} (%)[a]	0.075 (0.349)
Structure refinement	
Resolution (Å)	50–2.3 (2.38–2.30)
R_{cryst}/R_{free} (%)[b]	21.3 (25.5)/24.3 (31.9)
No. of reflections	
Working set	57726
Test set	2916
R_{msd} *from ideal values*	
Bond length (Å)	0.008
Bond angels (°)	1.2
Average B-factor (Å^2)	
Main chain	29.8
Side chain	32.3
No. of atoms	
Protein	5438
Ligand	78
Solvent (including waters, sulfate ions, and PEG molecules)	456
Ramachandran plot	
Most favored regions (%)	90.3
Additionally allowed (%)	8.7
Generously allowed (%)	1.0

Numbers in parentheses are for the highest resolution shell.
[a] $R_{merg} = \sum|I_i - I_m|/\sum I_i$, where I_i is the intensity of the measured reflection and I_m is the mean intensity of all symmetry-related reflections.
[b] $R_{cryst} = \sum||F_{obs}| - |F_{calc}||/\sum|F_{obs}|$, where F_{obs} and F_{calc} are observed and calculated structure factors. $R_{free} = \sum_T||F_{obs}| - |F_{calc}||/\sum_T|F_{obs}|$, where T is a test data set of about 10% of the total reflections randomly chosen and set aside prior to refinement.

model are good (Table 1). The *Li*OMT structure reveals a seven-stranded β sheet (β7 is anti-parallel to the other strands) with five helices on one side and three helices on the other side (Fig. 1a). This topology is consistent with the typical core fold of MTs except for two additional α helices at the N terminus (Martin and McMillan, 2002).

Homodimers are observed in the three-dimensional architecture of *Li*OMT as well as in solution, as demonstrated by size exclusion chromatography and sedimentation velocity experiment (data not shown). The dimerization interface buries 30% of the surface area in each monomer. Molecules A and C are related by a non-crystallographic 2-fold axis, whilst molecule B is related to another copy of B by the crystallographic 2-fold axis along *b*. The two dimmers are essentially the same with an RMSD of 0.65 Å when all the Cα are superimposed. The N-terminal loop, helices α1, α3 and β-strand β6 form the dimerization interface (Fig. 1b). Residues Lys4, Asn5, Glu13, Tyr15, Arg22, Glu47, Lsy57, Asn205, Try47, Lys57, Asn205, tyr209, and Asp215 are directly involved in the dimerization interactions. Residues from the N terminus until Glu13 insert into the partner molecule and are stabilized by the swapping-style interaction. N-terminal swapping is also observed in three other plant OMTs (chalcone *O*-methyltransferase, isoflavone *O*-methyltransferase, and caffeic acid/5-hydroxyferulic acid 3/5 *O*-methyltransferase), which have a small N-terminal domain involved in dimerization and formation of the back wall of the substrate-binding region (Zubieta et al., 2001, 2002). However, there is no N-terminal swapping in the CCoAOMT homodimer (Ferrer et al., 2005), and this dimerization style is seldom found in other structures of MTs.

3.2. Comparison with other OMTs

Each *Li*OMT molecule in the asymmetric unit binds a SAH molecule, which must have been co-purified with

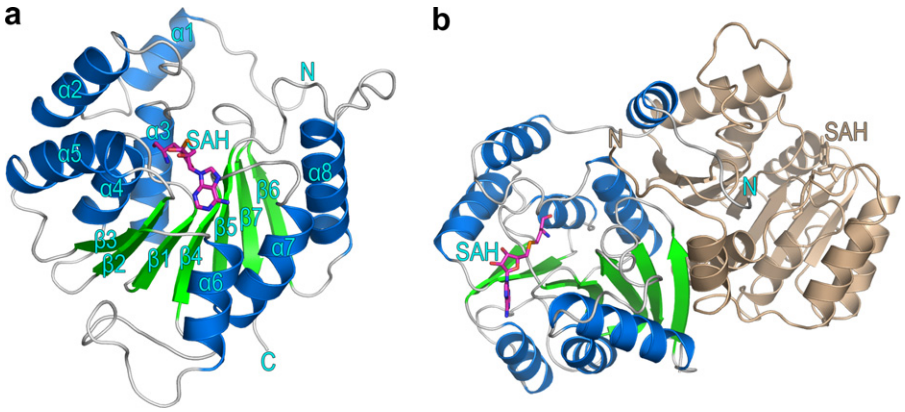

Fig. 1. Ribbon diagrams of the *Li*OMT three-dimensional architecture. (a) Ribbon diagram of the *Li*OMT monomer. The protein is colored by secondary structure (α helices is marine blue and β strands is green) elements and numbered from N terminus to the C terminus. The SAH molecule is shown as stick (carbon is slate; nitrogen is blue; oxygen is red; sulfur is orange). (b) Ribbon diagram of the *Li*OMT dimer. One monomer is colored as shown in (a), and the other is colored as wheat. This figure and Fig. 2b and c were prepared using the PyMol program (http://pymol.sourceforge.net/).

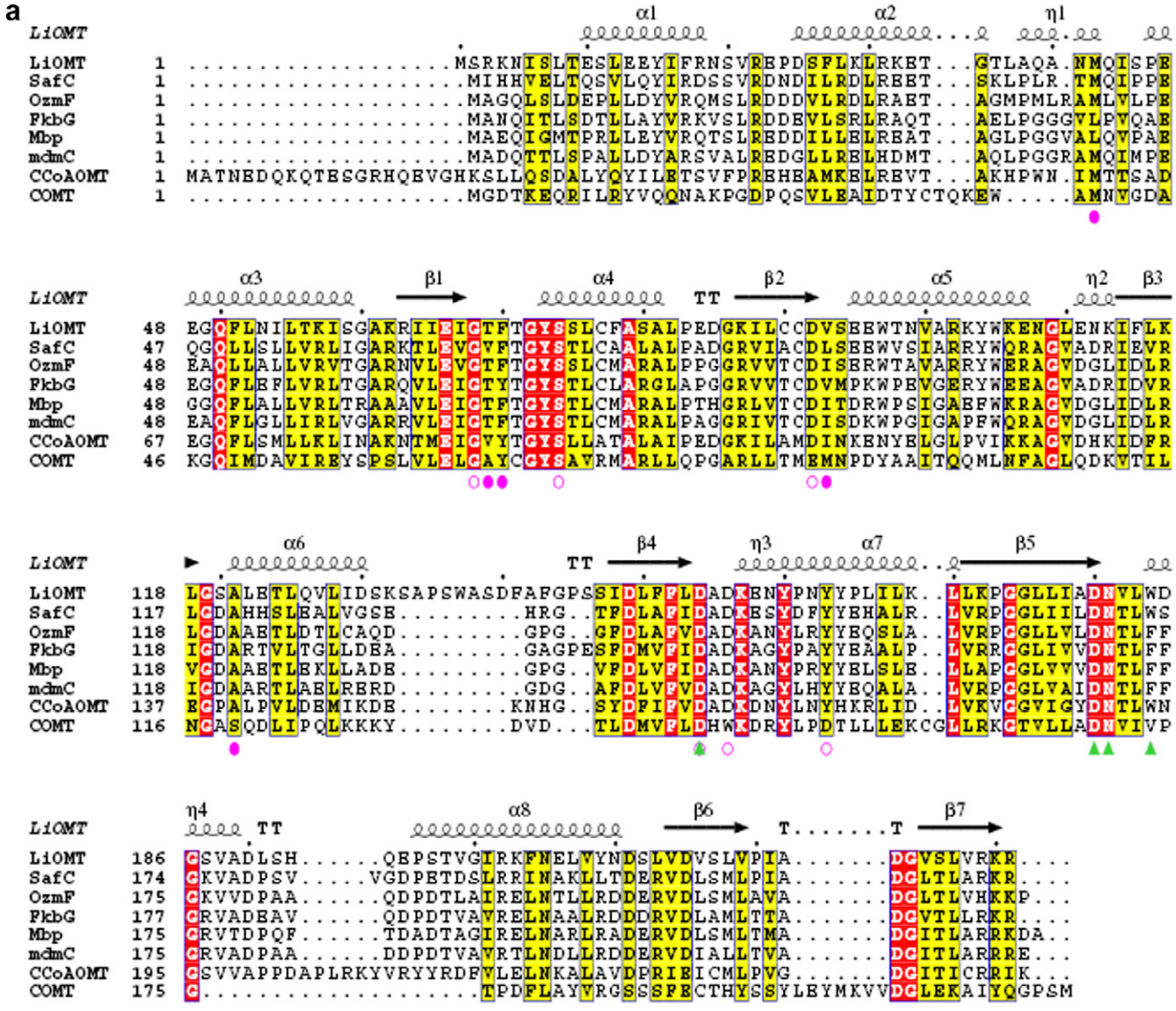
a
LiOMT
LiOMT
SafC
OzmF
FkbG
Mbp
mdmC
CCoAOMT
COMT
α1
α2
η1
α3
β1
α4
β2
α5
η2
β3
α6
β4
η3
α7
β5
η4
α8
β6
β7
b
c
Ser74
Glu66
Thr69
Phe70
Gly60
SAH
Asp154
Ca2+
Asp180
Asn181
Feruloyl CoA
Asp92
Met42
Ala121
Tyr163
Val93
Trp184
Asp156

*Li*OMT, since no SAH was added during expression, purification, and crystallization. The occupancies of SAH in molecule A and B were refined to 0.6 and SAH in molecule C seemed fully occupied. Accordingly, the electron density of Ala38–Aly40, which is close to SAH, is poor in molecule A and B but clear in molecule C. The implication is that the SAH molecule can stabilize the loop between α2 and α3 (residues Thr36–Ser45).

According to a DALI search for 3D structure similarity, *Li*OMT displays good agreement with CCoAOMT (PDB ID: 1SUI) from *Medicago sativa* (alfalfa) and COMT (PDB ID: 1VID) from rat. The sequence alignment and structural superposition of these three proteins are presented in Fig. 2a and b, respectively. *Li*OMT shows a highly conserved SAM (SAH) binding region, which is widely shared by a majority of MTs (Martin and McMillan, 2002). In *Li*OMT, the SAH-binding mode is similar to those in CCoAOMT and COMT. Gly68, Ser74, Asp92, Asp154, Asp156, and Tyr163 interact with the SAH molecule by hydrogen bonds. Met42, Thr69, Phe70, Val93, and Ala121 form hydrophobic interactions with SAH (Fig. 2c).

In the putative catalytic site opposite the SAH molecule, Asp154, Asp180, and Asn181 are proposed to be involved in the coordination of a divalent metal ion based on the structure of CCoAOMT and COMT (Fig. 2a). This divalent cation is believed essential for substrate-binding and hydroxyl orientation before the S_N2-like methylation reaction of some OMTs (Schubert et al., 2003). Asp154, Asp180, and Asn181 are conserved in *Li*OMT, adopting the similar conformations to those in CCoAOMT and COMT even though with no divalent cation binding (Fig. 2c). This suggests that *Li*OMT may share with above OMTs the same metal-dependent catalytic mechanism.

3.3. Implication of the possible substrate of LiOMT

The substrate of *Li*OMT remains unknown. However, in previously determined dimeric OMTs it was observed that the active site was pre-arranged upon SAM-binding, and the substrate did not trigger further conformational change (Zubieta et al., 2001, 2002; Ferrer et al., 2005). Therefore, the structure of *Li*OMT may provide useful information for its substrate specificity. In contrast to the conserved SAH-binding region and catalytic site, the substrate-binding region of *Li*OMT is noticeably different from that in CCoAOMT and COMT. In the structure of CCoAOMT complexed with the catalytic product, the N-terminal loop, the Loop between β5 and α8, and the short turn between β6 and β7 comprise the substrate-binding site. The N-terminal loop from the neighboring molecule (Arg3–Thr9; shown green in Fig. 2b) of *Li*OMT is structurally equal to the N-terminal loop of CCoAOMT and the extended loop between β6 and β7 in COMT, both of which embrace the substrate and work as the back wall of the substrate-binding region. The major divergence in the shape and size of the substrate-binding cavity comes from the loop between β5 and α8 (Fig. 2b). This loop in *Li*OMT is more open compared with those in CCoAOMT and COMT, leading to a larger substrate-binding region. In COMT structure, this loop is very short and the inhibitor 3,5-dinitrocatechol is intimately surrounded by the loops that comprise the substrate-binding region. In CCoAOMT, this loop protrudes to accommodate the long linear substrate feruloyl CoA. Hence, the tail of the substrate of *Li*OMT may be a large group due to the wide cavity produced by the loop between β5 and α8.

Analyzed by protein sequence similarity search (blastp on ExPASy against UniProt Knowledgebase), *Li*OMT shows good sequence similarity with five bacterial OMTs that are involved in antibiotic production. SafC from *M. xanthus* participates in the biosynthesis of the DNA-binding antibiotic and antitumor agent saframycin Mx1 (Pospiech et al., 1996), OzmF from *Streptomyces albus* is involved in the production of the hybrid peptide–polyketide antibiotic Oxazolomycin (Li et al., 2006), FkbG from *Streptomyces hygroscopicus* subsp. *ascomyceticus* is involved in the production of ascomycin (Wu et al., 2000), Methoxymalonate biosynthesis protein (for simplicity it will be referred as Mbp) from *Streptomyces neyagawaensis* is involved in the biosynthesis of macrolide concanamycin A (Haydock et al., 2005), and mdmC from *Streptomyces mycarofaciens* is responsible for the midecamycin production (Hara and Hutchinson, 1992) (Fig. 2a). *Li*OMT has greater similarity with the five bacterial OMTs in the loop between β5 and α8 that could be critical to the substrate specificity. SafC is the closest homolog to *Li*OMT amongst these OMTs of known function. It was proposed that the substrate of SafC should be a modified tyrosine in terms of cross-feeding experiment (Pospiech et al., 1996).

Fig. 2. (a) Sequence alignment of *Li*OMT with other OMTs. The OMTs including five bacterial OMTs (SafC from *Myxococcus xanthus*, OzmF from *Streptomyces albus*, FkbG from *Streptomyces hygroscopicus* subsp. *ascomyceticus*, Methoxymalonate biosynthesis protein (Mbp) from *Streptomyces neyagawaensis*, and mdmC from *Streptomyces mycarofaciens*), one plant OMT (CCoAOMT from alfalfa; PDB ID: 1SUI), and one animal OMT (soluble part of COMT from rat; PDB ID: 1VID) were aligned using ClustalW (Thompson et al., 1994). The alignment was based on structural alignment results to avoid gaps inside the conserved secondary structural elements. Defined by the analysis of the structure using DSSP program (Kabsch and Sander, 1983), the secondary structure of *Li*OMT is indicated above the alignment. The strictly conserved residues are shown in red boxes; similar residues are shown in yellow boxes. Residues involved in hydrogen bond interaction and hydrophobic interactions with SAH in *Li*OMT structure are marked by magenta circles which are hollow and solid, respectively. Residues involved in metal binding and substrate interaction are marked by green triangles. This figure was prepared with ESPript (Gouet et al., 1999). (b) Structural superposition of *Li*OMT (marine blue), CCoAOMT (pale yellow), and COMT (magenta). The structural alignment was obtained using Coot (Emsley and Cowtan, 2004). The N-terminal loop (residues Arg3–Thr9) from the neighboring monomers of *Li*OMT is presented as green. (c) Stick presentation of the SAH-binding site and putative catalytic site of *Li*OMT (marine blue) compared to the active site of CCoAOMT (pale yellow). Residue numbers of *Li*OMT are labeled as well as the calcium ion and the catalytic product feruloyl CoA of CCoAOMT.

Furthermore, Trp193 in CCoAOMT provides the hydrophobic interaction with the phenolic moiety of caffeoyl-CoA (Fig. 2c). Consistently, Trp184 of *Li*OMT is structurally equivalent to Trp193 of CCoAOMT and this residue is conserved as Trp or Phe in SafC and other similar bacterial methyltransferases. Therefore the substrate of *Li*OMT likely has a phenolic head that would be methylated and followed by a large, probably a ring-shaped moiety.

Another loop between α6 and β4 of *Li*OMT differs from other structures. The sequence of this loop is commonly observed in MTs from *Leptospira*. It is far away from the activity region and may be involved in the recognition of other proteins in the interaction network of *Leptospira*.

Coordinates

The atomic coordinates of the refined model of *Li*OMT have been deposited in RCSB Protein Data Bank under the accession number 2HNK.

Acknowledgments

We thank Dr. Yuhui Dong and Dr. Peng Liu in Institute of High Energy Physics and Mr. Yi Han in Institute of Biophysics for diffraction data collection. This work was supported by National Funding for Talent Youth (Grant No. 30225015), the 973 Program of the Ministry of Science and Technology (No. 2004CB720008), the National Natural Science Foundation of China (Grant No. 10490193) and the Chinese Academy of Sciences (KSCX1-YW-R-61).

References

Emsley, P., Cowtan, K., 2004. Coot: model-building tools for molecular graphics. Acta Crystallogr. D 60, 2126–2132.

Ferrer, J.L., Zubieta, C., Dixon, R.A., Noel, J.P., 2005. Crystal structures of alfalfa caffeoyl coenzyme A 3-*O*-methyltransferase. Plant Physiol. 137, 1009–1017.

Fontecave, M., Atta, M., Mulliez, E., 2004. *S*-adenosylmethionine: nothing goes to waste. Trends Biochem. Sci. 29, 243–249.

Gouet, P., Courcelle, E., Stuart, D.I., Metoz, F., 1999. ESPript: analysis of multiple sequence alignments in PostScript. Bioinformatics 15, 305–308.

Hara, O., Hutchinson, C.R., 1992. A macrolide 3-*O*-acyltransferase gene from the midecamycin-producing species *Streptomyces mycarofaciens*. J. Bacteriol. 174, 5141–5144.

Haydock, S.F., Appleyard, A.N., Mironenko, T., Lester, J., Scott, N., Leadlay, P.F., 2005. Organization of the biosynthetic gene cluster for the macrolide concanamycin A in *Streptomyces neyagawaensis* ATCC 27449. Microbiology 151, 3161–3169.

Kabsch, W., Sander, C., 1983. Dictionary of protein secondary structure: pattern recognition of hydrogen-bonded and geometrical features. Biopolymers 22, 2577–2637.

Laskowski, R., MacArthur, M., Moss, D., Thornton, J., 1993. PROCHECK: a program to check the stereochemical quality of protein structures. J. Appl. Crystallogr. 26, 283–291.

Li, W., Ju, J., Osada, H., Shen, B., 2006. Utilization of the methoxymalonyl-acyl carrier protein biosynthesis locus for cloning of the tautomycin biosynthetic gene cluster from *Streptomyces spiroverticillatus*. J. Bacteriol. 188, 4148–4152.

Martin, J.L., McMillan, F.M., 2002. SAM (dependent) I AM: the *S*-adenosylmethionine-dependent methyltransferase fold. Curr. Opin. Struct. Biol. 12, 783–793.

Murshudov, G.N., Vagin, A.A., Dodson, E.J., 1997. Refinement of macromolecular structures by the maximum-likelihood method. Acta Crystallogr. D 53, 240–255.

Otwinowski, Z., Minor, W., 1997. Processing of X-ray diffraction data collected in oscillation mode. Methods Enzymol. 276, 307–326.

Pospiech, A., Bietenhader, J., Schupp, T., 1996. Two multifunctional peptide synthetases and an *O*-methyltransferase are involved in the biosynthesis of the DNA-binding antibiotic and antitumour agent saframycin Mx1 from *Myxococcus xanthus*. Microbiology 142, 741–746.

Ren, S.X., Fu, G., Jiang, X.G., Zeng, R., Miao, Y.G., Xu, H., Zhang, Y.X., Xiong, H., Lu, G., Lu, L.F., Jiang, H.Q., Jia, J., Tu, Y.F., Jiang, J.X., Gu, W.Y., Zhang, Y.Q., Cai, Z., Sheng, H.H., Yin, H.F., Zhang, Y., Zhu, G.F., Wan, M., Huang, H.L., Qian, Z., Wang, S.Y., Ma, W., Yao, Z.J., Shen, Y., Qiang, B.Q., Xia, Q.C., Guo, X.K., Danchin, A., Saint Girons, I., Somerville, R.L., Wen, Y.M., Shi, M.H., Chen, Z., Xu, J.G., Zhao, G.P., 2003. Unique physiological and pathogenic features of *Leptospira interrogans* revealed by whole-genome sequencing. Nature 422, 888–893.

Schubert, H.L., Blumenthal, R.M., Cheng, X., 2003. Many paths to methyltransfer: a chronicle of convergence. Trends Biochem. Sci. 28, 329–335.

Storoni, L.C., McCoy, A.J., Read, R.J., 2004. Likelihood-enhanced fast rotation functions. Acta Crystallogr. D 60, 432–438.

Thompson, J.D., Higgins, D.G., Gibson, T.J., 1994. CLUSTAL W: improving the sensitivity of progressive multiple sequence alignment through sequence weighting, position-specific gap penalties and weight matrix choice. Nucleic Acids Res. 22, 4673–4680.

Vidgren, J., Svensson, L.A., Liljas, A., 1994. Crystal structure of catechol *O*-methyltransferase. Nature 368, 354–358.

Wu, K., Chung, L., Revill, W.P., Katz, L., Reeves, C.D., 2000. The FK520 gene cluster of *Streptomyces hygroscopicus var. ascomyceticus* (ATCC 14891) contains genes for biosynthesis of unusual polyketide extender units. Gene 251, 81–90.

Zhong, R., Iii, W.H., Negrel, J., Ye, Z.H., 1998. Dual methylation pathways in lignin biosynthesis. Plant Cell 10, 2033–2046.

Zubieta, C., He, X.Z., Dixon, R.A., Noel, J.P., 2001. Structures of two natural product methyltransferases reveal the basis for substrate specificity in plant *O*-methyltransferases. Nat. Struct. Biol. 8, 271–279.

Zubieta, C., Kota, P., Ferrer, J.L., Dixon, R.A., Noel, J.P., 2002. Structural basis for the modulation of lignin monomer methylation by caffeic acid/5-hydroxyferulic acid 3/5-*O*-methyltransferase. Plant Cell 14, 1265–1277.